Trakya University Journal of Engineering Sciences
http://dergipark.org.tr/tujes
ISSN 2147–0308

Research Article / Araştırma Makalesi
DOI: 10.59314/tujes.1736117

Constant Current Solution of a Memristor Modelled Using the Mutlu-Kumru Memristor Model and Two Possible Applications

Ertuğrul KARAKULAK[1]*, Reşat MUTLU[2]

[1] *Electronics Department, Vocational School of Technical Sciences, Tekirdağ Namık Kemal University, Tekirdag, Turkey*
[2] *Electrical and Electronics Engineering Department, Çorlu Engineering Faculty, Tekirdağ Namık Kemal University,*

Cite this article as: Karakulak, E., Mutlu, R., (2025). Constant Current Solution of a Memristor Modelled Using The Mutlu-Kumru Memristor Model And Two Possible Applications, *Trakya University Journal of Engineering Sciences*. 26(2), 77-90.

Highlights

- Simulation of the Mutlu-Kumru Window Function Based Memristor Model
- Sawtooth Signal Generator Simulation with the Mutlu-Kumru Memristor
- Sawtooth Signal Generator Analysis with the Mutlu-Kumru Memristor

Article Info

Article History:

Received:
July 6, 2025

Accepted:
December 30, 2025

Keywords:

Memristor;
Memristor Model;
Sawtooth Signal Generator;
Window Function;
Circuit Analysis.

Abstract

The Memristor is a novel and nonlinear circuit element. An analytical solution for the circuit it is part of does not always exist due to its nonlinearity. Also, since it is a new circuit element, the solutions of the memristor-based circuits should be examined. Memristors can be modeled using different approaches. A set of memristor models is called the nonlinear drift models, one of which, the Mutlu-Kumru model is one of the recently proposed. A memristor can be fed with a constant current source. However, its solution under a constant current source for the Mutlu-Kumru memristor model has not been presented in the literature, yet. In this study, the analytical solution of the Mutlu-Kumru memristor model under constant current excitation is presented. It is also demonstrated that the obtained solution can be utilized in analyzing resistive switching of a resistive memory and the modeling of a memristor-based sawtooth oscillator.

Mutlu-Kumru Memristör Modeli Kullanılarak Modellenen Bir Memristörün Sabit Akım Çözümü ve İki Olası Uygulama

Makale Bilgileri

Makale Tarihçesi:

Geliş:
6 Temmuz 2025

Kabul:
30 Aralık 2025

Anahtar Kelimeler:

Memristör;
Memristör Modeli;
Testere Dişi Sinyal Üreteci;
Pencere Fonksiyonu;
Devre Analizi.

Öz

Memristör, yeni ve doğrusal olmayan bir devre elemanıdır. Doğrusal olmaması nedeniyle, içinde bulunduğu devrenin analitik çözümü her zaman mevcut olmayabilir. Ayrıca, yeni bir devre elemanı olması sebebiyle memristör tabanlı devrelerin çözümlerinin incelenmesi gerekmektedir. Memristörler farklı yaklaşımlar kullanılarak modellenebilir. Memristör modellerinden bir grubu, doğrusal olmayan sürüklenme modelleri olarak adlandırılır ve bunlardan biri yakın zamanda önerilen Mutlu-Kumru modelidir. Bir memristör sabit bir akım kaynağı ile beslenebilir. Ancak, sabit akım kaynağı altında Mutlu-Kumru memristör modelinin çözümü henüz literatürde sunulmamıştır. Bu çalışmada Mutlu-Kumru memristör modelinin sabit akım uyartımı altındaki analitik çözümü sunulmaktadır. Ayrıca elde edilen çözümün rezistif belleklerin anahtarlanması ve memristör tabanlı testere dişi osilatörlerin modellenmesinde kullanılabileceği gösterilmektedir.

***Correspondence to:** ekarakulak@nku.edu.tr

1. Introduction

The concept of the memristor was proposed by Dr. Chua in 1971 (L. O. Chua, 1971). By 1976, memristive systems and their characteristics were diagnosed by Chua and Kang (L. O. Chua & Kang, 1976). In 2008, a thin film memristive system demonstrating memristor behavior was found by HP researchers (Strukov et al., 2008). Research on memristors and memristive systems has surged in the last two decades (Pershin et al., 2011; Prodromakis & Toumazou, 2010). New nanometer-scale materials exhibiting memristive properties are under research (Pershin & Di Ventra, 2011). Memristors are anticipated to play a nontraditional role in both analog and digital circuits (L. Chua, 2011; Prodromakis & Toumazou, 2010). Consequently, developing accurate memristor models is crucial (Khalid, 2019). Due to their non-linear properties, modeling the electrical characteristics of memristors remains challenging.

Memristors are closely related to resistive random-access memory (ReRAM) technologies, as resistive switching memories can be regarded as physical realizations of memristors (Chua, 2011). In ReRAM devices, the switching time between high- and low-resistance states is a key performance metric. While resistive switching has mostly been analyzed under constant voltage excitation (Strukov et al., 2008; Biolek et al., 2012; Mutlu & Kumru, 2023), constant current operation is also of practical importance for controlled switching and accurate determination of switching times. Therefore, analytical investigation of memristor models under constant current excitation is highly relevant for resistive memory applications.

Memristor models that incorporate window functions are widely used to represent memristors, and there are several types of window functions available in the literature (D. Biolek & Biolková, 2009; Eroğlu, 2017; Joglekar & Wolf, 2009; Khalid, 2019; Prodromakis et al., 2011; Strukov et al., 2008; Zha et al., 2016). The first window function was introduced by Strukov et al. (Strukov et al., 2008). Joglekar developed a shapeable nonlinear dopant drift memristor model, but it encounters issues with boundary handling (Joglekar & Wolf, 2009). Biolek et al. proposed a current direction-dependent window function that avoids boundary-handling issues (D. Biolek & Biolková, 2009). Prodromakis et al. introduced a scalable and shapeable window function, though it also faces boundary-handling problems (Prodromakis et al., 2011). This model has since been modified to address the boundary-handling issues and improve scalability (Zha et al., 2016). Some of these models are phenomenological in nature (Eroğlu, 2017; Khalid, 2019). Additionally, research (Mutlu & Kumru, 2023) has identified a boundary unreachability issue in certain memristor models, where they fail to switch within a finite time.

Memristors could enable the creation of programmable electronic circuits (Shin et al., 2009, 2011). They can also be used to design electronically programmable amplifiers (Berdan, R.; Prodromakis, T.; Pershin & Di Ventra, 2010; T. a. Wey & Jemison, 2011). Research has explored the use of memristors in filters (Ascoli et al., 2013; S. C. Yener et al., 2018; Ş. Ç. Yener et al., 2014), and they are also applicable for developing phase shifters or modulator circuits (Mutlu, R., Karakulak, 2018; T. A. Wey & Benderli, 2009). Studies In (Itoh & Chua, 2008; Muthuswamy, 2010) have investigated memristor-based chaotic oscillators, while (Mosad et al., 2013; Fauda, 2015; Çakır et al., 2025; S. Ç. Yener et al., 2014; Talukdar et al. 2011), present various types of memristor-based relaxation oscillators.

A memristor-based sawtooth signal generator (MBSSG) is proposed and analyzed both analytically and experimentally using an HP memristor emulator (Özgüvenç et al., 2016). Additionally, other memristor models featuring nonlinear drift speed are employed to simulate the MBSSG (Kurtdemir A.; Mutlu R., 2019).

It is demonstrated that the memristor models discussed in MBSSG (Kurtdemir A.; Mutlu R., 2019). Face issues with boundary handling or boundary reachability, except for the HP memristor model (Mutlu & Kumru, 2023). Although simulations of the MBSSG are presented in (Kurtdemir A.; Mutlu R., 2019), the nonlinear dopant drift memristor models are unable to accurately complete the resistive switching analytically, leading to incorrect simulations (Mutlu & Kumru, 2023).

The model developed by Kumru and Mutlu is suitable for modeling the MBBSG because it performs resistive switching in both forward and reverse polarities, like the HP memristor. Some LTspice models for memristors are documented in the literature (D. Biolek & Biolková, 2009; Karakulak & Mutlu, 2020). An LTspice model of the proposed memristor model has been used to examine a memristor-capacitor (M-C) parallel circuit, though this model was not included in (Mutlu & Kumru, 2023). Presenting this LTspice model is crucial as it does not encounter boundary handling or unreachability issues. The study aims to analyze the MBSSG using this new model, provide its LTspice representation (Mutlu & Kumru, 2023), and employ it for simulating the MBSSG.

The memristor represents a novel addition to circuit components, and solutions for its interactions with other elements are not always straightforward. The Reference (Joglekar & Wolf, 2009) provides an overview of various memristor properties. (Joglekar & Wolf, 2009) and (Mutlu, 2015) examines series TiO2 memristor-capacitor circuits operating without an external power source. (Bayır & Mutlu 2013) examines a memristor-Inductor Series Circuit fed by a constant voltage source with memristor being modeled with a PWL function.

HP Joglekar and Prodromakis window functions are used in the memristor-based circuit analysis in (Dautovic et al., 2024; Radwan et al., 2010; Biolek et al. 2012). An exact solution for memristor-based circuits is not always possible (Yener et al., 2018; Yener et al, 2014). Sometimes such solutions may require Taylor series or transcendental functions such as Lambert W function (Yener et al, 2014; Sozen & Cam, 2014; Urgan et al., 2020).

The mathematical modeling of memristors and the analysis of memristor-based circuits are significant research topics due to their nonlinear dynamic behavior. Various memristor models have been proposed in the literature, each representing specific physical and mathematical characteristics. Among these, the Mutlu-Kumru model was recently developed as an alternative approach that addresses some deficiencies found in existing models. It has been shown that the Mutlu-Kumru memristor model can do resistive switching under constant current voltage excitation (Mutlu & Kumru, 2023). However, studies on the analytical solution of the memristor models under a constant current source remain quite limited. This study presents the analytical solution of the Mutlu-Kumru memristor model under a constant current source and provides two application examples based on the obtained solution. It is demonstrated that the solution can be utilized in switching resistive RAMs and in the modeling of memristor-based sawtooth oscillators.

This paper is organized as follows: The second section provides a brief overview of the Mutlu-Kumru memristor model. The third section gives the solution of a memristor fed by a constant current source for both polarities using the Mutlu-Kumru memristor model. In the fourth section, two application examples of this analysis, a resistive memory and a sawtooth signal generator circuit are provided. The results of the analytical model of the sawtooth signal generator are compared to these simulation results obtained with LTspice simulations. The paper concludes with the final section.

2. Mutlu-Kumru Memristor Model

Some thin films, which exhibit zero-crossing current-voltage hysteresis loops that change with frequency, are classified as memristive systems and are commonly referred to as memristors today. The following equations present a memristor model that incorporates nonlinear dopant drift.

$$v(t) = R(x)i(t) \tag{1}$$

$$\frac{dx}{dt} = \mu_v \frac{R_{on}}{D^2} i(t) f(x,i) \tag{2}$$

where $R(x)$ represents the resistance of the memristor, $i(t)$ denotes its current, $v(t)$ indicates its voltage, w is the length of its oxidized region, μ_v is the dopant mobility, D is the total length of the TiO_2 region, $x = w/D$ is the normalized oxidized length, R_{on} is the minimum resistance, and $f(x,i)$ is the window function.

The memristance of the memristor which is its state-variable dependent resistance is given as

$$R(x) = R_{off} - (R_{off} - R_{on})x \tag{3}$$

where $\boldsymbol{R_{on}}$ and $\boldsymbol{R_{off}}$ represent the minimum and the maximum values of the memristance.

Its memristance can vary between $\boldsymbol{R_{on}}$ and $\boldsymbol{R_{off}}$.

A window function reflects how closely a memristive system approximates an ideal memristor (D. Biolek & Biolková, 2009). The memristive state-variable or resistance value changes only when the window function $f(x,i)$ is non-zero. According to (Mutlu & Kumru, 2023), certain established models also encounter a problem known as boundary reachability, where the memristive switching time becomes infinite in both polarities. To address this, a new window function that takes device polarity into account is proposed. Considering shapeability in both directions, the Mutlu-Kumru memristor model is given as

$$f(x,i) = m_1 \sqrt[n_1]{1-x}\, stp(i) + m_2 \sqrt[n_2]{x}\, stp(-i). \tag{4}$$

or

$$f(x,i) = \begin{cases} m_1 \sqrt[n_1]{1-x}, & i \geq 0 \\ m_2 \sqrt[n_2]{x}, & i < 0 \end{cases}. \tag{5}$$

where n_1 and n_2 are the shaping parameters used to determine the shape the window function for the forward and reverse polarities respectively, m_1 and m_2 are scaling parameters to control the height of the window function for the forward and reverse polarities respectively.

A memristor model that employs this window function changes states within a finite duration when a DC voltage is applied (Mutlu & Kumru, 2023). Combining Eq.s (1-4) makes the new memristor model. By unifying Equations (1-4), The Mutlu-Kumru memristor model is obtained. Figure 1 displays the Mutlu-Kumru window functions for both forward and reverse polarities. The shaping parameters n_1 and n_2 determine the shape of these window functions. Additional details about the model are available in (Mutlu & Kumru, 2023).

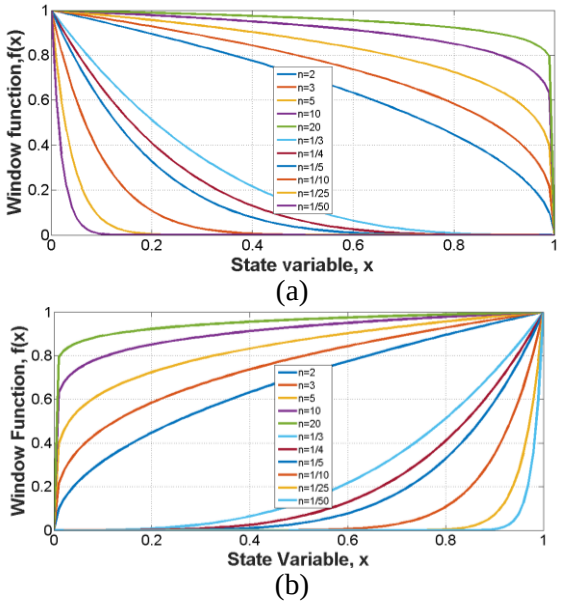

Figure 1. Window function of the Mutlu-Kumru memristor a) the forward biased memristor ($i(t)>0$), 10 n_1 values, and $m_1=1$ and b) the reverse biased memristor ($i(t)<0$), 10 n_2 values, and $m_2=1$. (Mutlu & Kumru, 2023).

Figure 2 displays the LTspice block diagram of the memristor model. The memristor is modeled as a three-terminal circuit element implemented as a subcircuit.

Two of these terminals represent the memristor connections, while the third terminal (*XSV*) is used for plotting the state variable. Within the subcircuit, a current source and a capacitor are configured to compute the memristor's state variable. The current sources, denoted as *Gmem* and *Gx*, are identical, which enables the calculation of the charge flow through the memristor. Detailed LTspice code for the memristor model can be found in the study (Karakulak & Mutlu, 2024).

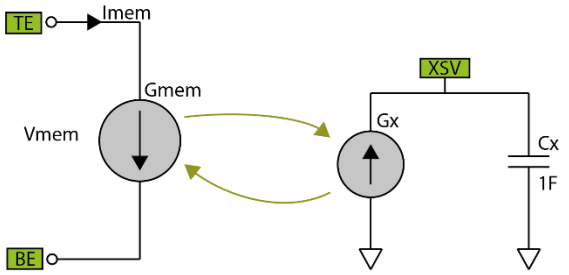

Figure 2. Block Scheme of the Memristor Model

The memristor model is excited with a 50 Hz 2 V sinusoidal signal. Figure 3 shows the results of the simulation. It presents the memristor voltage, memristor current, and state variable. Detailed LTspice simulation results and hysteresis curves of the memristor model can be found in (Karakulak & Mutlu, 2024).

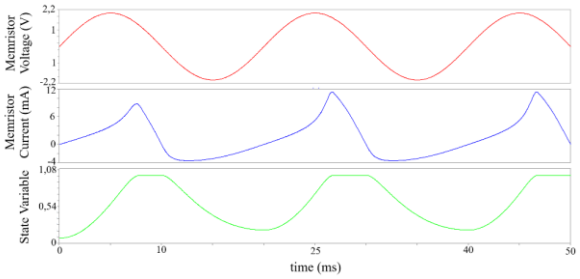

Figure 3. Voltage, current and state variable of the Mutlu-Kumru memristor model (Ron=150Ω, R_{off}=1000Ω, μ_v=40.10^{-15} m^2/Vs, D= 16 nm, m_1=2, m_2=3, n_1=2, n_2=2)

3. Analysis of a Memristor Fed by a Current Source with Mutlu-Kumru Window Function

A memristor supplied by a constant current source by opening the switch S at $t = t_0$ is shown in Figure 4. The memristance and the voltage of the memristor depends on the memristor's state variable $x(t)$ varying with respect to time. If the memristor current is positive, i.e., it is forward-biased, and equal to I_p,

$$i(t) = I_P > 0. \tag{6}$$

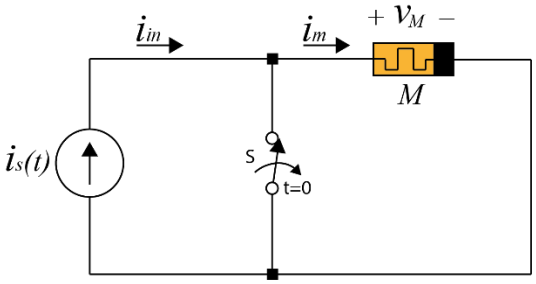

Figure 4. A memristor supplied by a current source.

The state variable $x(t)$ can be solved using Eq. (2):

$$\frac{dx}{dt} = \mu_v \frac{R_{on}}{D^2} I_p f(x,i) \tag{7}$$

$$\frac{dx}{dt} = \frac{\mu_v R_{on}}{D^2} I_p m_1 \sqrt[n_1]{1-x} \tag{8}$$

$$\frac{\mu_v R_{on} I_p m_1}{D^2} \int_{t_0}^{t} dt = \int_{x(0)}^{x(t)} \frac{dx}{\sqrt[n_1]{1-x}}. \tag{9}$$

$$\frac{\mu_v R_{on} I_p m_1}{D^2}(t-t_0) = \int_{x(0)}^{x(t)} (1-x(t))^{-1/n1} dx = \frac{\left((1-x(0))^{1-\frac{1}{n_1}} - (1-x(t))^{1-\frac{1}{n_1}}\right)}{\left(1-\frac{1}{n_1}\right)} \tag{10}$$

$$(1-x(t))^{1-\frac{1}{n_1}} = (1-x(0))^{1-\frac{1}{n_1}} - \left(1-\frac{1}{n_1}\right)\frac{\mu_v R_{on} I_p m_1}{D^2}(t-t_0) \tag{11}$$

$$x(t) = 1 - \sqrt[1-\frac{1}{n_1}]{(1-x(0))^{1-\frac{1}{n_1}} - \left(1-\frac{1}{n_1}\right)\frac{\mu_v R_{on} I_p m_1}{D^2}(t-t_0)} \tag{12}$$

If the switching occurs in the forward direction, the state variable becomes equal to 1 and stays constant since the polarity does not change:

$$x(t) = 1. \tag{13}$$

In this case,

$$R(x) = R_{on}. \tag{14}$$

$$v(t) = R(x)i(t) = R_{on}I_P. \tag{15}$$

If the memristor current is negative, i.e., it is reverse-biased, and equal to $-I_n$. Then,

$$i(t) = -I_n < 0, \tag{16}$$

The state variable $x(t)$ can be solved using Eq. (2):

$$\frac{dx}{dt} = -\frac{\mu_v R_{on}}{D^2} I_n m_2 \sqrt[n_2]{x} \tag{17}$$

$$-\frac{\mu_v R_{on} I_n m_2}{D^2}\int_{t_0}^{t} dt = \int_{x(t_0)}^{x(t)} \frac{dx}{\sqrt[n_2]{x}}. \tag{18}$$

$$-\frac{\mu_v R_{on} I_n m_2}{D^2}(t-T) = \int_{x(t_0)}^{x(t)} \big(x(t)\big)^{-\frac{1}{n_2}} dx = \frac{\left((x(t))^{1-\frac{1}{n_2}} - (x(t_0))^{1-\frac{1}{n_2}}\right)}{\left(1-\frac{1}{n_2}\right)}$$

$$-\frac{\mu_v R_{on} I_n m_2}{D^2}\int_{t_0}^{t} dt = \int_{x(t_0)}^{x(t)} \frac{dx}{\sqrt[n_2]{x}}. \tag{19}$$

$$-\frac{\mu_v R_{on} I_n m_2}{D^2}\left(1-\frac{1}{n_2}\right)\int_{t_0}^{t} dt = (x(t))^{1-\frac{1}{n_2}} - \big(x(t_0)\big)^{1-\frac{1}{n_2}}$$

$$(x(t))^{1-\frac{1}{n_2}} = -\frac{\mu_v R_{on} I_n m_2}{D^2}\left(1-\frac{1}{n_2}\right)\int_{t_0}^{t} dt + (x(t_0))^{1-\frac{1}{n_2}} \tag{20}$$

$$x(t) = \sqrt[1-\frac{1}{n_2}]{(x(t_0))^{1-\frac{1}{n_2}} - \left(1-\frac{1}{n_2}\right)\frac{\mu_v R_{on} I_n m_2}{D^2}(t-t_0)} \tag{21}$$

If the switching occurs in the reverse direction, the state variable becomes equal to 0 and stays constant since the polarity does not change:

$$x(t) = 0. \tag{22}$$

$$R(x) = R_{off}. \tag{23}$$

$$v(t) = R(x)i(t) = -R_{off}I_n. \tag{24}$$

4. Analysis and Simulations of the Model and Sawtooth Generator Circuit

It is important to know how to analyze the sawtooth generator with the proposed memristor model. In this section, the analytical solution and simulation examples of the generator are given.

4.1. Switching Times of a Memristive Memory with a Current Source

Resistive switching memories are regarded as memristors by Chua (Chua, 2011). In (Mutlu & Kumru, 2023), the resistive switching time of some well-known memristor models and the Mutlu-Kumru model have been examined by making resistive switching with a DC voltage source. If a constant current source instead of a constant voltage source is used to switch the state of a memristive memory, it can be worth examining what the resistive switching times would be.

Applying a positive current pulse I_p and using Eq. (21), the resistive switching time of the forward-biased memristor, the forward polarity resistive switching time, which is the time needed x(t) going from 0 to 1, is found as:

$$\frac{\mu_v R_{on} I_p m_1}{D^2}\tau_{SWP} = \int_0^1 (1-x)^{-1/n_1} dx = \frac{\left((1-0)^{1-\frac{1}{n_1}} - (1-1)^{1-\frac{1}{n_1}}\right)}{\left(1-\frac{1}{n_1}\right)} \tag{25}$$

The switching time is given as

$$\tau_{SWP} = \frac{D^2}{\mu_v R_{on} I_P m_1\left(1-\frac{1}{n_1}\right)} \tag{26}$$

If the switching occurs in the forward direction, the state variable becomes equal to 1 and stays constant since the polarity does not change. Eq.s (14) and (15) are valid in this case.

If the state variable switches from 1 to 0, using a negative current pulse $-I_n$, the resistive switching time of the reverse-biased memristor is found as

$$-\frac{\mu_v R_{on} I_n m_2}{D^2}\tau_{SWN} = \int_1^0 (x)^{-1/n_2} dx = \frac{\left((0)^{1-\frac{1}{n_2}} - (1)^{1-\frac{1}{n_2}}\right)}{\left(1-\frac{1}{n_2}\right)} \quad (27)$$

$$\tau_{SWN} = \frac{D^2}{\mu_v R_{on} I_n m_2 \left(1-\frac{1}{n_2}\right)} \quad (28)$$

After the switching occurs in the reverse direction, i.e., for $t \geq \tau_{SWN}$, the state variable becomes equal to zero and stays constant if the voltage polarity does not change. Eq.s (23) and (24) are valid in this case.

4.2 Analysis of the Sawtooth Generator with Mutlu-Kumru Window Function

The memristor-based sawtooth signal generator (MBSSG) presented in (Özgüvenç et al, 2016; Kurtdemir & Mutlu, 2019; Karakulak & Mutlu, 2020; Karakulak & Mutlu, 2024) is shown in Figure 5.a. It comprises a relaxation oscillator and an inverting amplifier that has a memristor used as the feedback component. The purpose of the relaxation oscillator is to produce a square wave. In Figure 5.b, the memristor polarity is selected so that its memristance increases with a positive current. The square wave results in Opamp drawing a square wave current. A memristor's memristance increases in the positive alternance and decreases in the negative alternance if the memristor is not under saturation, i.e., its state variable is varying. In this case, the output of the MBSSG generator is negative memristor voltage. If the memristor is under saturation, i.e., its state variable is constant, the output of the MBSSG generator becomes constant, too.

The solutions that were given with most of the window functions (Kurtdemir & Mutlu, 2019) are not valid due to boundary-tackling and boundary unreachability issues reported in (Joglekar & Wolf, 2009; Mutlu & Kumru, 2023). The Mutlu-Kumru memristor model has not been used to analyze the signal generator yet.

The output voltage of the relaxation generator can be assumed to be

$$,V_{in} = \begin{cases} V_{sat}, & 0 < t < \frac{T}{2} \\ -V_{sat}, & \frac{T}{2} < t < T \end{cases} \quad (29)$$

where V_{sat} is the saturation voltage of the Opamp of the relaxation oscillator and T is the electrical period of the square wave and equal to 1/f.

The frequency of the relaxation oscillator is given as

$$f = \frac{0.455}{R_f C} \quad (30)$$

where R_f and C are the resistance and the capacitance of the negative feedback part of the relaxation oscillator.

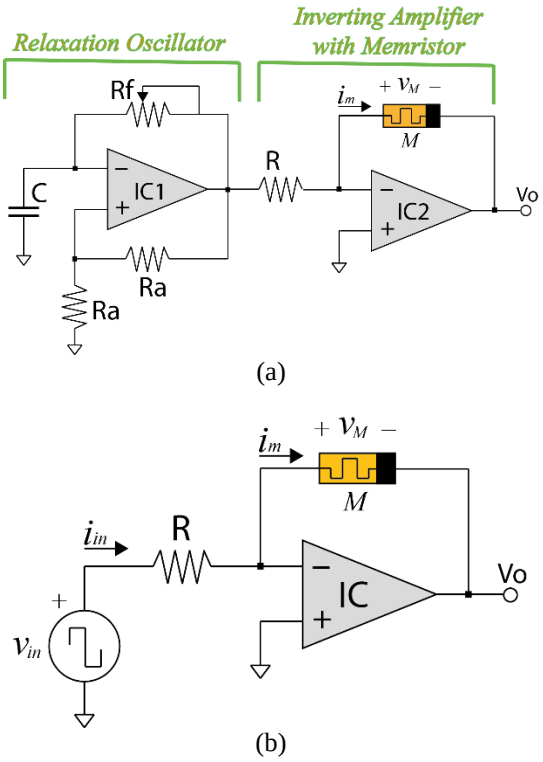

Figure 5. The sawtooth wave generator with a memristor (Özgüvenç et al, 2016).

The input current of the R-M amplifier which is also the memristor current can be calculated as

$$I_{in} = i(t) = \frac{V_{in}}{R} = \begin{cases} \frac{V_{sat}}{R}, & 0 < t < \frac{T}{2} \\ -\frac{V_{sat}}{R}, & \frac{T}{2} < t < T \end{cases} \quad (31)$$

where R is the input resistance of the inverting amplifier.

Renaming $I_{dc} = \frac{V_{sat}}{R}$, the memristor of the R-M amplifier or the memristor can be regarded as being fed by a square current source:

$$I_{in} = i(t) = \begin{cases} I_{dc}, & 0 < t < \frac{T}{2} \\ -I_{dc}, & \frac{T}{2} < t < T \end{cases} \quad (32)$$

The output voltage of the MBSSG is equal to

$$V_{out} = -\frac{R(x)}{R}.V_{in} \quad (33)$$

$$V_{out} = -\frac{\left(R_{off} - \left(R_{off} - R_{on}\right)x(t)\right)}{R}.V_{in} \quad (34)$$

The output voltage of the MBSSG depends on the memristor state variable $x(t)$ with respect to time. It can be solved using Eq. (2):

$$\frac{dx}{dt} = \mu_v \frac{R_{on}}{D^2}.\frac{V_{sat}}{R} f(x,i) \quad (35)$$

For the forward-biased memristor, $V_{in} > 0$ or $\frac{T}{2} > t > 0$,

$$\frac{dx}{dt} = \frac{\mu_v R_{on} V_{sat}}{RD^2} m_1 \sqrt[n_1]{1-x} \quad (36)$$

$$\frac{\mu_v R_{on} V_{sat} m_1}{RD^2} \int_0^t dt = \int_{x(0)}^{x(t)} \frac{dx}{\sqrt[n_1]{1-x}}. \quad (37)$$

$$\frac{\mu_v R_{on} V_{sat} m_1}{RD^2} t = \int_{x(0)}^{x(t)} (1-x(t))^{-1/n1} dx = \frac{\left((1-x(0))^{1-\frac{1}{n_1}} - (1-x(t))^{1-\frac{1}{n_1}}\right)}{\left(1-\frac{1}{n_1}\right)} \quad (38)$$

$$(1-x(t))^{1-\frac{1}{n_1}} = (1-x(0))^{1-\frac{1}{n_1}} - \left(1-\frac{1}{n_1}\right)\frac{\mu_v R_{on} V_{sat} m_1}{RD^2} t \quad (39)$$

$$x(t) = 1 - \sqrt[1-\frac{1}{n_1}]{(1-x(0))^{1-\frac{1}{n_1}} - \left(1-\frac{1}{n_1}\right)\frac{\mu_v R_{on} V_{sat} m_1}{RD^2} t} \quad (40)$$

If the state variable switches from 0 to 1, the forward polarity resistive switching time is given as

$$\frac{\mu_v R_{on} V_{sat} m_1}{RD^2} \tau_{SWP} = \int_0^1 (1-x)^{-1/n_1} dx = \frac{\left((1-0)^{1-\frac{1}{n_1}} - (1-1)^{1-\frac{1}{n_1}}\right)}{\left(1-\frac{1}{n_1}\right)} \quad (41)$$

The switching time is given as $\tau_{SWP} = \frac{RD^2}{\mu_v R_{on} V_{sat} m_1 \left(1-\frac{1}{n_1}\right)}$ (42)

After the switching occurs in the forward direction, i.e., for $T/2 \geq t \geq \tau_{SWP}$, the state variable becomes equal to 1 and stays constant if the voltage polarity does not change. In this case,

$$x(t) = 1. \quad (43)$$

$$R(x) = R_{on}. \quad (44)$$

$$i(t) = \frac{V_{sat}}{R(x)} = \frac{V_{sat}}{R_{on}}. \quad (45)$$

And the output voltage is given as

$$V_{out} = -\frac{R_{on}}{R}.V_{in}. \quad (46)$$

84ort he reverse-biased memristor, i.e., $i(t) < 0$, $V_{in} = -V_{sat} < 0$ or $\frac{T}{2} < t < T$,

$$\frac{dx}{dt} = -\frac{\mu_v R_{on} V_{sat}}{RD^2} m_2 \sqrt[n_2]{x} \quad (47)$$

$$-\frac{\mu_v R_{on} V_{sat} m_2}{RD^2} \int_{T/2}^t dt = \int_{x(T/2)}^{x(t)} \frac{dx}{\sqrt[n_2]{x}}. \quad (48)$$

$$-\frac{\mu_v R_{on} V_{sat} m_2}{RD^2}\left(t-\frac{T}{2}\right)=\int_{x(0)}^{x(t)}\left(x(t)\right)^{-\frac{1}{n_2}}dx=\frac{\left(\left(x(t)\right)^{1-\frac{1}{n_2}}-\left(x\left(\frac{T}{2}\right)\right)^{1-\frac{1}{n_2}}\right)}{\left(1-\frac{1}{n_2}\right)}$$

$$-\frac{\mu_v R_{on} V_{sat} m_2}{RD^2}\int_{T/2}^{t} dt=\int_{x(T/2)}^{x(t)}\frac{dx}{\sqrt[n_2]{x}}. \quad (49)$$

$$-\frac{\mu_v R_{on} V_{sat} m_2}{RD^2}\left(1-\frac{1}{n_2}\right)\left(t-\frac{T}{2}\right)=\left(x(t)\right)^{1-\frac{1}{n_2}}-\left(x\left(\frac{T}{2}\right)\right)^{1-\frac{1}{n_2}}$$

$$\left(x(t)\right)^{1-\frac{1}{n_2}}=-\frac{\mu_v R_{on} V_{sat} m_2}{RD^2}\left(1-\frac{1}{n_2}\right)\left(t-\frac{T}{2}\right)+\left(x(T/2)\right)^{1-\frac{1}{n_2}} \quad (50)$$

$$x(t)=\sqrt[1-\frac{1}{n_2}]{\left(x(T/2)\right)^{1-\frac{1}{n_2}}-\left(1-\frac{1}{n_2}\right)\frac{\mu_v R_{on} V_{sat} m_1}{RD^2}\left(t-\frac{T}{2}\right)} \quad (51)$$

If the state variable switches from 0 to 1 in the negative half period, the resistive switching time is given as

$$-\frac{\mu_v R_{on} V_{sat} m_2}{RD^2}\tau_{SWN}=\int_1^0 (x)^{-1/n_2}dx=\frac{\left((0)^{1-\frac{1}{n_2}}-(1)^{1-\frac{1}{n_2}}\right)}{\left(1-\frac{1}{n_2}\right)} \quad (52)$$

$$\tau_{SWN}=\frac{RD^2}{\mu_v R_{on} V_{sat} m_2\left(1-\frac{1}{n_2}\right)} \quad (53)$$

After the switching occurs in the reverse direction, i.e. for $T \geq t - T/2 \geq \tau_{SWN}$, the state variable becomes equal to zero and stays constant if the voltage polarity does not change:

$$x(t)=0. \quad (54)$$

$$R(x)=R_{off}. \quad (55)$$

$$i(t)=-\frac{V_{sat}}{R(x)}=-\frac{V_{sat}}{R_{off}}\ . \quad (56)$$

LTspice circuit presentation of the MBSSG is given in Figure 6 and it is analyzed using the Mutlu-Kumru memristor model made in the last section. The memristor and the circuit parameters used in the simulations are given in Table 1. For these parameters, the memristor current, the memristor state variable, the memristor, the memristor current, the memristor state variable, the memristor, the memristor, the memristor state variable, and the output voltage waveforms are simulated at 24 Hz and presented in Figures 7 and 8.

Table 1. Circuit element parameters used in the simulations

The memristor minimum resistance	R_{on}	150 Ω
The memristor maximum resistance	R_{off}	1000 Ω
The dopant mobility	μ_v	40.10^{-15} $m^2/V.s$
The memristive element length	D	16 nm
Parameter m_1	m_1	2
Parameter m_2	m_2	3
Parameter n_1	n_1	2
Parameter n_2	n_2	2
Opamp	U_2	OP7
Inverting Amplifier Resistor	R_2	400 Ω

At high frequencies, the sawtooth signal generator produces an almost sawtooth waveform as shown in the previous study (Karakulak & Mutlu, 2024). As shown in Figures 7 and 8, the 24 Hz operation frequency is low enough for the memristor to get into saturation since its voltage becomes constant in some intervals in each period. Due to the operation of the memristor in the saturation region, the output voltage is not a good sawtooth waveform. The memristor's state variable switches from 0 to 1 or 1 to 0 if the half period of the square wave signal is higher than the resistive switching time as shown in Figures 7 and 8. The analytical solution presented here can predict these behaviors accurately as shown in Figures 7 and 8. The shape of the output waveform of the generator can be optimized by adjusting its frequency or using different memristor parameters and using the solution provided here.

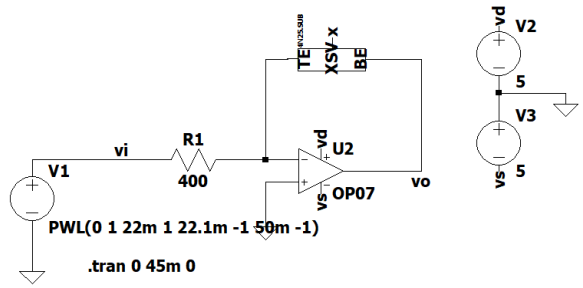

Figure 6. The LTspice schematic of the inspected generator.

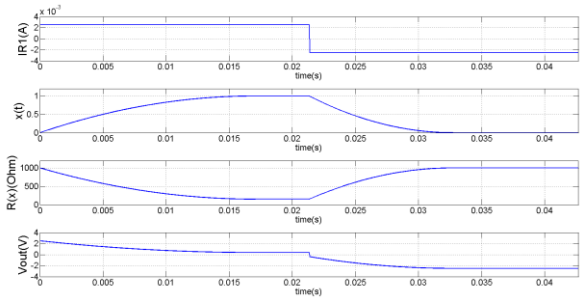

Figure 7. Simulation results of Matlab code of the sawtooth generator circuit.

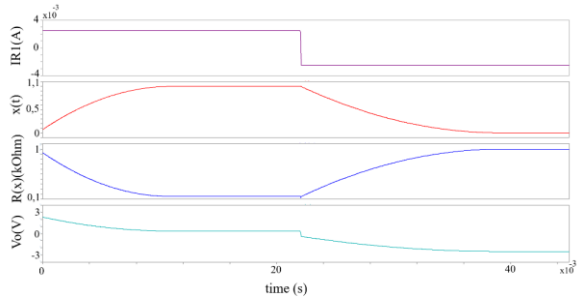

Figure 8. LTspice simulation results of the sawtooth generator circuit.

5. Results and Discussion

The analytical solution derived for the Mutlu–Kumru memristor model under constant current excitation was validated using LTspice simulations. The analytical expressions accurately describe the nonlinear evolution of the memristor state variable and terminal voltage for both current polarities. As observed throughout the simulations, the analytical and numerical results are in very good agreement, confirming the validity of the proposed solution for circuit-level analysis.

When the duration of the applied current exceeds the resistive switching time imposed by the window function of the Mutlu–Kumru model, the memristor enters the saturation region. In this case, the state variable reaches its boundary values and the terminal voltage remains nearly constant over part of the excitation period. The analytical solution allows direct calculation of these switching times. Due to the symmetric structure of the model and the constant magnitude of the applied current, the positive and negative switching times are equal to each other, which is also confirmed by the simulation results.

Figures 7 and 8 present the time-domain response of the memristor-based sawtooth signal generator operating at a low frequency of 24 Hz. These figures are particularly important because they clearly illustrate the effect of saturation and explain the deviation from an ideal sawtooth waveform. For a square-wave current excitation and the selected memristor polarity, when the current is positive, the memristor state variable $x(t)$ increases from 0 to 1 and reaches saturation at approximately 15 ms. After this point, $x(t)$ remains constant until the end of the positive half-period. During this interval, the memristance decreases from its maximum value to its minimum value, causing the output voltage to decrease accordingly.

In the negative half-period of the square-wave current, the behavior is reversed. The state variable decreases from 1 to 0, while the memristance increases from its minimum value back to its maximum value. Thus, while (x(t)) increases, the memristance decreases during the positive current interval, and the opposite behavior occurs during the negative current interval. Since the input current is a square wave, the output voltage waveform directly follows the time variation of the memristance.

The differences observed in Figures 7 and 8 compared to high-frequency operation arise from the fact that, at 24 Hz, the half-period of the excitation is sufficiently long for the memristor to fully switch within each cycle. As a result, saturation intervals appear in the voltage waveform, preventing the formation of an ideal

sawtooth shape. At higher frequencies, the memristor does not reach its boundary states within a half-period, and a nearly ideal sawtooth waveform is obtained. The analytical solution accurately predicts these behaviors and explains the physical origin of the waveform distortion.

Overall, the close agreement between analytical predictions and simulation results demonstrates that the proposed solution provides an effective and reliable tool for analyzing resistive switching behavior and the dynamic operation of memristor-based oscillators.

6. Conclusion

New circuit elements require analytical solutions to be used in the design of electrical and electronic circuits.

The Mutlu-Kumru memristor model has a window function, which allows finite resistive switching times. In this paper, an analytical solution of a memristor fed by a constant current source is presented. Then, the solution is used to calculate the switching times of a resistive memory and analyze a memristor-based sawtooth signal generator whose memristor is modeled with the Mutlu-Kumru memristor model. The analytical solution of the sawtooth signal generator has also been shown to exist. The solutions can be used to design oscillator circuits like the one given here.

In the future, once memristors are commercially available, it may be feasible to develop various types of signal generators based on various memristors. They will require analytical solutions for a good design. The experience given here can be used to design similar types of circuits with different memristor models. The solutions given here are also important from a circuit theory point of view.

Conflict of Interest: The authors declare no conflict of interest to be disclosed.

ORCID

Ertuğrul Karakulak : 0000-0001-5937-2114

Reşat Mutlu : 0000-0003-0030-7136

References

Ascoli, A., Tetzlaff, R., Corinto, F., Mirchev, M., & Gilli, M. (2013). Memristor-based filtering applications. LATW 2013 - 14th IEEE Latin-American Test Workshop, 1, 1–6. https://doi.org/10.1109/LATW.2013.6562672

Bayır, Ö., & Mutlu, R. (2013). Investigation of Memristor-Inductor Series Circuit under DC Excitation Using a Piecewise Memristor Characteristic, 6. İleri Muhendislik Teknolojileri Sempozyumu, 25-26.

Berdan, R.; Prodromakis, T.; Toumazou, C. (2012). High precision analogue memristor state tuning. Electronics Letters, 48(18), 1105–1107.

Biolek, D., & Biolková, V. (2009). SPICE Model of Memristor with Nonlinear Dopant Drift. Radioengineering, 18(2), 210–214.

Biolek, Z., Biolek, D., & Biolkova, V. (2012). Analytical solution of circuits employing voltage-and current-excited memristors. IEEE Transactions on Circuits and Systems I: Regular Papers, 59(11), 2619-2628.

Chua, L. (2011). Resistance switching memories are memristors. Applied Physics A, 102(4), 765–783. https://doi.org/10.1007/s00339-011-6264-9

Chua, L. O. (1971). Memristor—The Missing Circuit Element. IEEE Transactions on Circuit Theory, 18(5), 507–519. https://doi.org/10.1109/TCT.1971.1083337

Chua, L. O., & Kang, S. M. (1976). Memristive Devices and Systems. Proceedings of the IEEE, 64(2), 209–223. https://doi.org/10.1109/PROC.1976.10092

Çakır, K., Mutlu, R., & Karakulak, E. (2025). A memristor-based Liénard Oscillator design. Journal of the Faculty of Engineering and Architecture of Gazi University, 40(2), 1183-1195.

Dautovic, S., Samardzic, N., Juhas, A., Ascoli, A., & Tetzlaff, R. (2024). Analytical Solutions for Charge and Flux in HP Ideal Generic Memristor Model with Joglekar and Prodromakis Window Functions. IEEE Access.

Eroğlu, Y. O. A. F. G. A. H. (2017). A new window function for memristor modeling. 8th International Adbanced Technologies Symposium, 3498–3502.

Fouda, Mohammed E.; RADWAN, Ahmed G. (2015). Power dissipation of memristor-based relaxation oscillators. Radioengineering, 24(4), 968-973.

Itoh, M., & Chua, L. O. (2008). Memristor oscillators. International Journal of Bifurcation and Chaos, 18(11), 3183–3206. https://doi.org/10.1142/S0218127408022354

Joglekar, Y. N., & Wolf, S. J. (2009). The elusive memristor: Properties of basic electrical circuits. European Journal of Physics, 30(4), 661–675. https://doi.org/10.1088/0143-0807/30/4/001

Karakulak, E., & Mutlu, R. (2020). Spice model of current polarity-dependent piecewise linear window function for memristors. Gazi University Journal of Science, , 33(4), 766–777. https://doi.org/10.35378/gujs.605118

Karakulak, E., & Mutlu, R. (2024). SPICE Model of Mutlu-Kumru Memristor Model and Its Usage for Analysis, Modeling, And Simulation of a Memristor-Based Sawtooth Signal Generator. Trakya Üniversitesi Mühendislik Bilimleri Dergisi, 25(2), 91-100.

Khalid, M. (2019). Review on Various Memristor Models, Characteristics, Potential Applications, and Future Works. Transactions on Electrical and Electronic Materials, 20(4), 289–298. https://doi.org/10.1007/s42341-019-00116-8

Kurtdemir A.; Mutlu R. (2019). Modeling and Simulation of a Memristor-Based Sawtooth Signal Generator Using Nonlinear Dopant Drift Memristor Models. European Journal of Engineering and Applied Sciences, 2(1), 44–57.

Mosad, a. G., Fouda, M. E., Khatib, M. a., Salama, K. N., & Radwan, a. G. (2013). Improved memristor-based relaxation oscillator. Microelectronics Journal, 44(9), 814–820. https://doi.org/10.1016/j.mejo.2013.04.005

Muthuswamy, B. (2010). Implementing memristor based chaotic circuits. International Journal of Bifurcation and Chaos, 20(5), 1335–1350. https://doi.org/10.1142/S0218127410026514

Mutlu, R., Karakulak, E. (2018). Memristor-Based Phase Shifter. 2018 2nd International Symposium on Multidisciplinary Studies and Innovative Technologies (ISMSIT), 1–5.

Mutlu, R. (2015). Solution of TiO2 memristor-capacitor series circuit excited by a constant voltage source and its application to calculate operation frequency of a programmable TiO2 memristor-capacitor relaxation oscillator. Turkish Journal of Electrical Engineering and Computer Sciences, 23(5), 1219–1229. https://doi.org/10.3906/elk-1108-38

Mutlu, R., & Kumru, T. D. (2023). A Zeno Paradox: Some Well-known Nonlinear Dopant Drift Memristor Models Have Infinite Resistive Switching Time. Radioengineering, 32(3), 312–324. https://doi.org/10.13164/RE.2023.0312

Özgüvenç, A., Mutlu, R., & Karakulak, E. (2016). Sawtooth signal generator with a memristor. 1st International Conference on Engineering Technology and Applied Sciences, April, 19–24.

Pershin, Y. V., & Di Ventra, M. (2010). Practical approach to programmable analog circuits with memristors. IEEE Transactions on Circuits and Systems I: Regular Papers, 57(8), 1857–1864. https://doi.org/10.1109/TCSI.2009.2038539

Pershin, Y. V., & Di Ventra, M. (2011). Memory effects in complex materials and nanoscale systems. In Advances in Physics (Vol. 60, Issue 2, pp. 145–227). https://doi.org/10.1080/00018732.2010.544961

Pershin, Y. V., Martinez-Rincon, J., & Di Ventra, M. (2011). Memory circuit elements: From systems to applications. Journal of Computational and Theoretical Nanoscience, 8(3), 441–448. https://doi.org/10.1166/jctn.2011.1708

Prodromakis, T., Peh, B. P., Papavassiliou, C., & Toumazou, C. (2011). A versatile memristor model with nonlinear dopant kinetics. IEEE Transactions on Electron Devices, 58(9), 3099–3105. https://doi.org/10.1109/TED.2011.2158004

Prodromakis, T., & Toumazou, C. (2010). A review on memristive devices and applications. 2010 IEEE International Conference on Electronics, Circuits, and Systems, ICECS 2010 - Proceedings, 934–937. https://doi.org/10.1109/ICECS.2010.5724666

Radwan, A. G., Zidan, M. A., & Salama, K. N. (2010, August). HP memristor mathematical model for periodic signals and DC. In 2010 53rd IEEE International Midwest Symposium on Circuits and Systems (pp. 861-864). IEEE.

Shin, S., Kim, K., & Kang, S. M. (2009). Memristor-based fine resolution programmable resistance and its applications. 2009 International Conference on Communications, Circuits and Systems, ICCCAS 2009, 948–951. https://doi.org/10.1109/icccas.2009.5250376

Shin, S., Kim, K., & Kang, S. M. (2011). Memristor applications for programmable analog ICs. IEEE Transactions on Nanotechnology, 10(2), 266–274. https://doi.org/10.1109/TNANO.2009.2038610

Sozen, H., & Cam, U. (2014). First-order memristor–capacitor filter circuits employing hp memristor. Journal of Circuits, Systems, and Computers, 23(08), 1450116.

Strukov, D. B., Snider, G. S., Stewart, D. R., & Williams, R. S. (2008). The missing memristor found. Nature, 453(7191), 80–83. https://doi.org/10.1038/nature06932

Talukdar, A., Radwan, A. G., & Salama, K. N. (2011). Generalized model for Memristor-based Wien family oscillators. Microelectronics Journal, 42(9), 1032–1038. https://doi.org/10.1016/j.mejo.2011.07.001

Urgan, N. N., Dalmış, C., & Mutlu, R. (2020). Analysis of the HP Memristor and Capacitor (MC) Series Circuit Using the Lambert W Function. European Journal of Engineering and Applied Sciences, 3(2), 27-32.

Wey, T. A., & Benderli, S. (2009). Amplitude modulator circuit featuring TiO2 memristor with linear dopant drift. Electronics Letters, 45(22), 1103–1104. https://doi.org/10.1049/el.2009.2174

Wey, T. a., & Jemison, W. D. (2011). Variable gain amplifier circuit using titanium dioxide

memristors. IET Circuits, Devices & Systems, 5(1), 59. https://doi.org/10.1049/iet-cds.2010.0210

Yener, S. Ç., Mutlu, R., & Kuntman, H. (2014). A new memristor-based high-pass filter/amplifier: Its analytical and dynamical models. 2014 24th International Conference Radioelektronika, RADIOELEKTRONIKA 2014 - Proceedings. https://doi.org/10.1109/Radioelek.2014.6828420

Yener, S. C., Mutlu, R., & Kuntman, H. H. (2018). Small signal analysis of memristor-based low-pass and high-pass filters using the perturbation theory. Optoelectronics and Advanced Materials, Rapid Communications, 12(1–2), 55–62.

Yener, Ş. Ç., Mutlu, R., & Kuntman, H. H. (2014). Performance analysis of a memristor - Based biquad filter using a dynamic model. Informacije MIDEM, 44(2), 109–118.

Zha, J., Huang, H., & Liu, Y. (2016). A Novel Window Function for Memristor Model with Application in Programming Analog Circuits. IEEE Transactions on Circuits and Systems II: Express Briefs, 63(5), 423–427. https://doi.org/10.1109/TCSII.2015.2505959